Journal of Chromatography, 629 (1993) 361–370
Elsevier Science Publishers B.V., Amsterdam

CHROM. 24 658

Calibration of spectrophotometric detectors for supercritical fluid chromatography

U. Meier and Ch. Trepp

Institute of Process Engineering and Cryogenics, Swiss Federal Institute of Technology, ETH Zentrum, CH-8092 Zurich (Switzerland)

(First received July 23rd, 1992; revised manuscript received October 2nd, 1992)

ABSTRACT

A simple peak-area calibration method for supercritical fluid chromatography (SFC) with spectrophotometric detectors is presented. The method was developed originally for high-performance liquid chromatography and is based on the molar absorptivity of the analytes. It allows calibration independent of detector specifications, flow cell geometry and operating parameters. The adaptation of this method to SFC and the particular influence of the density variations of the highly compressible SFC eluent on calibration and reproducibility of results are discussed. SFC hardware requirements and operational and calibration procedures that are prerequisites for accurate quantitative SFC results were considered. The method was tested with samples of fatty acid glycerol esters, α-tocopherol (vitamin E) and its acetate in carbon dioxide–ethanol eluents with two different UV detectors. Errors and shortcomings of the method that narrow the scope of its applications are discussed.

INTRODUCTION

In the literature published on supercritical fluid chromatography (SFC), only a few papers have dealt with quantification other than by internal standard methods. The latter, however, require the addition of a known amount of a standard substance to the sample solution. The chosen standard substance should behave in a way similar to that of the sample constituents as far as retention and detection properties are concerned. It is not always possible, however, to find such a standard substance or to mix it with the sample in a reproducible way. This applies in the particular situation where SFC is directly coupled to the source of the sample, *e.g.*, in systems with on-line supercritical fluid extraction (SFE) of the sample [1] or, as in our case, where SFC is directly coupled with a high-pressure equilibrium cell for phase composition measurements [2]. In these situations it is highly desirable to have a method that links the integrated peak areas with the total number of sample molecules, irrespective of detector type, flow cell geometry and operating parameters of the SFC equipment.

Such a method was presented by Torsi *et al.* [3] for applications in high-performance liquid chromatography (HPLC) and tested experimentally with different UV–Vis detectors [4]. They found that their method worked well for some commercial UV detectors (three out of five), whereas others showed deviations of up to 20%. These were explained by deflections of the light beam at the flow cell caused by either wedged flow cell windows or non-ideal flow causing density gradients across the flow cell diameter. Peck and Morris [5] investigated such effects. They found window wedge angles of up to 2° for commercial flow cells and made photographs of tracer flow patterns in the cell, which exhibit considerable deviation from a constant distribution of sample substance across the width of the light beam. These effects are held responsible for baseline drifts and excess noise of the detector signal.

Correspondence to: U. Meier, Institute of Process Engineering and Cryogenics, Swiss Federal Institute of Technology, ETH Zentrum, CN-8092 Zurich, Switzerland.

0021-9673/93/$06.00

SFC exhibits some particular features that distinguish it from HPLC: the dense gas eluents are much more compressible than the liquid solvents used in HPLC. Spectroscopic detectors (UV–Vis, IR, fluorescence) for SFC operate at pressures up to 350 bar, which may affect the optical properties of the flow cells. As a further complication, SFC requires back-pressure control devices for releasing the system pressure after the detector. The use of passive restrictors [6] results in pressure-dependent flow, which is unacceptable in many instances, especially if absolute quantification is required. Active control valves are difficult to find or to build for the small flow-rates of the dense gas eluent, particularly if packed microbore or capillary columns are used. The method presented here requires the determination of the volume flow-rate of the eluent in the detector flow cell, which is simple in HPLC but more complex in SFC, because the SFC eluent density inside the flow cell depends on pressure, temperature and composition (if mixed eluents or modifiers are used).

Some aspects of the following theory have been presented before (in relation to HPLC). However, to the authors' knowledge, these have never been integrated into an applicable calibration method for SFC, and the effects of major changes in eluent density have not been treated.

In this paper we discuss the following theoretical aspects: Lambert–Beer law, the effect of SFC eluent density changes on peak shapes and integrated peak areas and non-plug flow in the detector flow cells. The validity of the theory is checked against standard calibration procedures, the measurement and control facilities required for application of the method are described and the problems arising are discussed.

THEORY

The Lambert–Beer law relates light absorbance, A, to the concentration of the absorbing molecules in the light path, c (mol/l), their molar absorptivity, ε ($\times 1000\ \mathrm{cm^2/mol}$) and the length of the light path, l_0 (cm). Considering that in chromatography A and c are time dependent, we can write

$$A_\lambda(t) \equiv \log (I_0/I)_\lambda = \varepsilon_\lambda\, l_0\, c(t) \qquad (1)$$

The deduction of this law assumes that sample concentrations are small [6] and that solvent effects on sample spectra are unimportant.

Chromatographic detectors determine the light intensity I_0 at the start of a run, thus taking the initial absorbance of the eluent without any sample present as the datum value. Problems may arise if short wavelengths are chosen (<210 nm), where end absorption of SFC eluents increases, particularly if they contain modifiers. In such cases there may not be enough energy available for proper measurements; artefacts result, as will be shown in the results for the calibration of oleic acid glycerides.

An ideal detector requires either an exactly parallel light beam passing through its flow cell, or a constant refractive index inside the cell, at least during one chromatographic run [4,5]. Parallelism of light beams depends on the optical set-up and is hardly ever fully accomplished, whereas constancy of refractive index depends on constant density and constant composition of the eluent. If density is to be constant, no temperature, pressure or modifier concentration programming is allowed in SFC. Changing the density would create detector baseline drifts and/or disturb quantitation. Temperature constancy of the flow cell is very important, but badly neglected in the design of many commercial HPLC and SFC detectors. Refractive index fluctuations due to sample peak concentration variations cannot be avoided. According to Peck and Morris [5], no ideal mixing takes place in conventional flow cells, such that peaks will always cause a certain increase in signal noise.

There are several effects of changing the SFC eluent density. First, it determines the solubility and miscibility of modifiers and samples. Increasing density normally enhances solubilities. As high-pressure phase equilibria are complex, care has to be taken not to operate in the two-phase region. Failure to do so would result in unexpected and irreproducible behaviour of the chromatographic system. Phase behaviour of the binary system carbon dioxide–ethanol was reported by Panagiotopoulos and Reid [7]. It exhibits a marked influence of temperature on the immiscibility gap, particularly at low ethanol concentrations (up to 10% ethanol). At 50 C at least 120 bar are required to keep clear of the two-phase region.

The second effect of density is in changing the shape of sample peaks. With a density decrease due

to eluent temperature rising along the flow path (e.g., in the detector), the volume of a peak carrying the sample expands accordingly, and the maximum of the local peak concentration function $c(x)$ falls while the peak width increases.

The third effect of density is in changing the flow velocity of the eluent. A rise in temperature will increase the velocity, in proportion to the decrease in density, decreasing the residence time of sample molecules in the detector flow cell. Consequently, peak widths of the time-dependent concentration function $c(t)$ "seen" by the detector [when a given peak $c(x)$ passes through] decrease.

The point of interest is in knowning the resulting composite effect of density on the peak area determined by integrating the detector signal $A(t)$. Expansion of the peak width is compensated for by the increase in the flow velocity, so that the peak width in terms of time remains unaffected by an increase in density. The decrease in the local concentration maximum, however, is not compensated for. We therefore expect that integrated peak areas, a_i, will change proportionally with eluent density in the detector flow cell, ρ_{fc}:

$$a_i = \int_{peak} A(t)\mathrm{d}t \approx \rho_{fc} \quad \text{(s)} \tag{2}$$

The third element of the method is the concept of residence time distribution in the flow cell and its effect on the measured optical absorbance. If the flow cell is considered as a closed vessel of any geometry and any flow pattern, being swept by a steady-state flow of eluent of constant density, then the concentration profile of any peak measured at the inlet, $c(t)$, can be related to its profile at the outlet, $c_{out}(t)$, by any normalized exit age distribution funcion $E(t)$ [8] by the following equation:

$$c_{out}(t) = \int_0^t c(t')\ E(t-t')\mathrm{d}t' \quad \text{(mol/l)} \tag{3}$$

where t' is a dummy variable running from 0 to t. $E(t'')$ has the following properties:

$$\int_0^\infty E(t'')\mathrm{d}t'' = 1; \quad \int_0^t E(t'')\mathrm{d}t'' \equiv F(t); \quad \int_t^\infty E(t'')\mathrm{d}t'' = 1 - F(t) \tag{4}$$

$F(t)$ is the fraction of fluid that remains in the vessel for a time shorter than t. Levenspiel [8] showed that $F(t)$ is the normalized outlet response of a step function at the vessel inlet. Further, we define a function $R(t'')$:

$$R(t'') \equiv 1 - F(t'')$$

with

$$\int_0^\infty R(t'')\mathrm{d}t'' = \tau = \frac{V}{\dot{V}} \quad \text{(s)} \tag{5}$$

This is the same R function as used, but not explained, by Torsi and co-workers [3,4]. The integral under the R function curve is equal to the mean residence time τ of fluid flowing through the vessel (volume V) at a given flow-rate.

With these tools we can now determine the number of sample molecules n_{fc} present in the flow cell volume V_{fc} from the peak concentration profile at the inlet, $c(t)$, and the residence time distribution function $E(t'')$. With $c_{fc}(t)$ being the average concentration in the flow cell at any time t, we obtain

$$n_{fc}(t) = V_{fc}\ c_{fc}(t) = \dot{V}\int_0^t c(t')\left(\int_{(t-t')}^\infty E(t'')\mathrm{d}t''\right)\mathrm{d}t' \quad \text{(mol)} \tag{6}$$

The inner integral represents that fraction of the sample which entered the flow cell at any time $t' < t$ and remains in the flow cell longer than $t - t'$. With eqns. 4 and 5, eqn. 6 is rewritten as

$$n_{fc}(t) = \dot{V}\int_0^t c(t')[1 - F(t-t')]\mathrm{d}t' = \dot{V}\int_0^t c(t')\ R(t-t')\mathrm{d}t' \quad \text{(mol)} \tag{7}$$

With the rules for Laplace transformations, this so-called "convolution integral" can be integrated to yield a product of separate and simple integrals:

$$\int_0^\infty n_{fc}(t) = V_{fc}\int_0^\infty c_{fc}(t)\mathrm{d}t = \dot{V}\int_0^\infty c(t)\mathrm{d}t\int_0^\infty R(t)\mathrm{d}t = n_{peak}\tau \quad \text{(mol s)} \tag{8}$$

where n_{peak} is the total number of moles injected with the sample and conveyed in the peak.

It is important to note that the deduction of this equation did not require any assumption concerning ideal flow patterns in the flow cell. It is therefore generally valid for constant density, steady-state flow through a closed flow cell. Assuming that all of the sample molecules present in the cell are illumi-

nated by the detector light beam, and that the assumptions of the Lambert–Beer law (eqn. 1) are fulfilled, we find a simple relationship between integrated peak areas and the amount of sample:

$$a_i = \int_0^\infty A_\lambda(t)\mathrm{d}t = \frac{\varepsilon_\lambda\, l_0\, n_{peak}}{\dot{V}} = \frac{\varepsilon_\lambda\, l_0\, n_{peak}\, \rho_{fc}}{\dot{m}} \quad \text{(s)} \quad (9)$$

We find that in addition to the amount of sample and its molar absorptivity, the length of the light path, the mass flow-rate and the density of the eluent in the flow cell determine the integrated peak area, which corresponds to the qualitative considerations leading to the proportionality eqn. 2.

Eqn. 9 is rearranged in order to define a calibration factor that ideally is equal to the molar absorptivity of the sample:

$$e_\lambda \equiv \left(\frac{a_i\, \dot{m}}{l_0\, n_{peak}\, \rho_{fc}}\right)_{meas.} \approx \varepsilon_\lambda \quad (10)$$

It follows that the parameters in eqns. 9 and 10 must be known accurately and be controlled reproducibly in order to be able to use the molar absorptivity for detector calibration in SFC. We explain below how we achieved this goal experimentally.

EXPERIMENTAL

The SFC system developed during this work is shown in Fig. 1. It was built for the purpose of direct measurement of high-pressure equilibrium phase compositions.

The first aim is to achieve constant, reproducible and pulse-free flow. For that purpose, an Isco 260D syringe pump is used to deliver liquid carbon dioxide (99.99%, recondensed from vapour) at constant pressure. A second, similar pump (Isco μLC500, constant volume flow-rate mode) delivers ethanol (puriss., 99.8%) as the polar modifier. Mixing occurs in a simple tee-fitting, followed by a piece of coiled capillary tubing. For the purpose of temperature adjustment these are immersed in the same water-bath that contains the two high-pressure sample injection valves.

The valves used are motor-driven Valco C6W (2 μl, for light equilibrium phase) and Valco C14W (0.06 μl, for heavy equilibrium phase), followed by a third valve for injection of calibration solutions (Valco C6W, 20 μl, with automatic filling system).

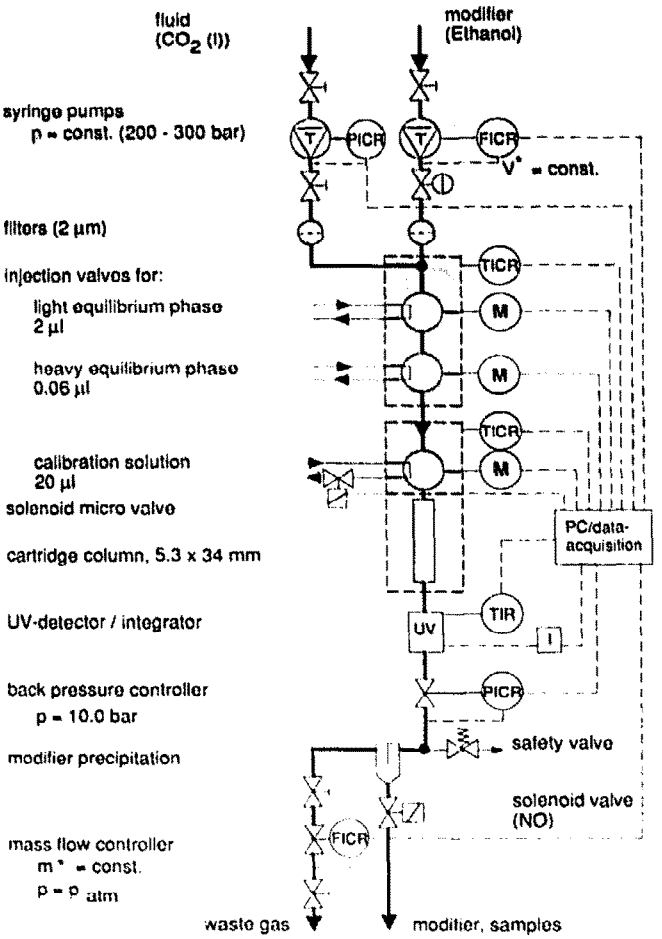

Fig. 1. Flow diagram of supercritical fluid chromatograph (shaded: temperature-controlled areas).

This last valve is kept at the column temperature (typically 30 °C) by a metal block thermostat.

A short cartridge column with Nucleosil 100-3 packing (unmodified spherical silica, 3 μm particle diameter, 100 Å pore diameter, packing dimensions 34 mm × 5.3 mm diameter) separates the sample components. It allows for typical run times as short as 1–5 min.

The UV detectors used are a Perkin-Elmer LC235 (35 diode-array) and an Isco V4 (variable-wavelength). A Perkin-Elmer LC1100 integrator is used to integrate peak areas.

The second important element for achieving constant flow is the pressure release valve. A Brooks 5835P high-pressure control valve (k_{vs} value $2 \cdot 10^{-5}$, orifice diameter 0.051 mm) with electronic

back-pressure controller and pressure transducer reduces the pressure to 10 bar, thus avoiding the formation of solid carbon dioxide. The modifier is precipitated at this pressure and a Brooks 5850E mass-flow controller releases the carbon dioxide (with small amounts of modifier vapour) to atmospheric pressure.

The system is remote controlled by a personal computer (Olivetti M24) with data acquisition hardware (Burr-Brown PCI 20000). The software is written in Turbo Pascal and allows the measurement, storage and statistical evaluation of all the important SFC parameters (pressures, temperatures, flow-rates), on-line calculation and display of non-measurable system parameters (such as eluent density in the detector flow cell) and time-controlled chromatographic runs at constant intervals.

The parameters in eqn. 9 were determined in the following ways.

The length of the flow cell optical light path, l_0, was taken from the manufacturer's specifications, as we were not in a position to measure it at the operating pressures. According to Torsi *et al.* [4], however, deviations from nominal values of several percent may occur.

The sample amount, n_{peak}, was determined with calibration substances from Sigma, dissolved in UV-grade heptane. Impurities in the calibration substances used, inaccuracies of the weighing balance and evaporation of the solvent contribute to composite errors. The volumes of the injection valve sample loops may deviate widely from nominal values. It was therefore determined by filling the loop with mercury, switching the valve, flushing the loop with compressed air and consequently weighing the ejected mercury. For small volumes several consecutive fill–eject cycles were combined into one weighing to increase accuracy (results are given in Table I).

The density of the eluent in the flow cell, ρ_{fc}, was initially measured at different pressures, temperatures and ethanol concentrations by means of a Paar DMA 512 high-pressure/high-temperature oscillating tube densitometer cell. Later it was calculated on-line from measured values of flow cell temperature, pressure and eluent flow-rate. Flow cell temperature was measured by means of a thermocouple and pressure was determined from the value measured at the pump (which was checked regularly by a dead-weight gauge), diminished by the system pressure drop calculated from eluent flow-rates by means of an empirical correlation. This pressure drop was always smaller than 30 bar.

The mass flow-rate of the eluent was determined from the signals of the mass-flow controller (carbon dioxide mass flow-rate, calibrated regularly by means of a laboratory wet test meter) and of the ethanol pump (ethanol volume flow-rate).

TABLE I

NOMINAL AND MEASURED SAMPLE LOOP VOLUMES OF SOME HPLC INJECTION VALVES USED IN THIS WORK

Loop No.	Type[a]	Nominal volume (μl)	Volume measured (μl)	S.D.[b] (μl)	R.S.D.[b] (%)	Deviation from nominal value (%)
1	E	20	20.484	0.053	0.26	+2.4
2	E	10	10.713	0.071	0.67	+7.1
3	E	5	6.117	0.031	0.50	+22.3
4	E	2	1.995	0.027	1.38	−0.3
5	I	1	0.606	0.0154	2.54	−39.4
6	I	0.5	0.540	0.0115	2.14	+8.0
7	I	0.2	0.180	0.0082	4.56	−10.0
8	I	0.06	0.06281	0.00095	1.52	+4.7

[a] E = External loop; I = internal loop.
[b] $n = 10$.

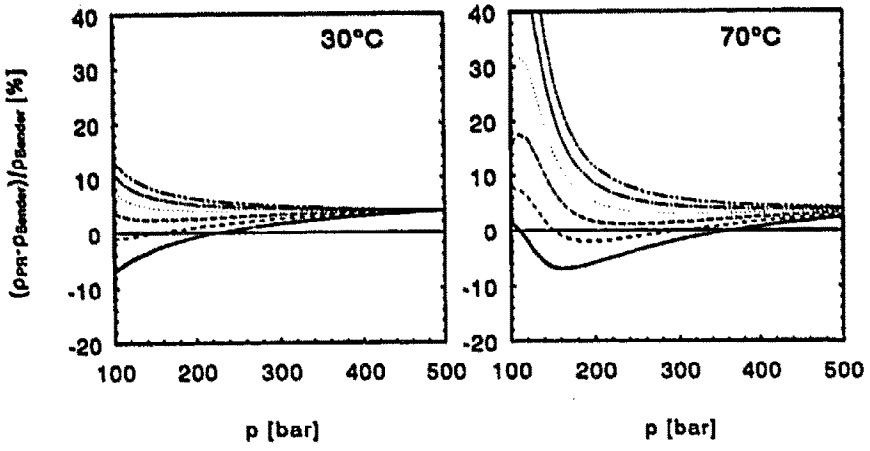

Fig. 2. CO_2–ethanol density: deviation of values calculated with Peng–Robinson EOS from values determined with Bender EOS (pure CO_2). Ethanol content (%): ——— = 0; ··· = 2; – – – = 4; · · · · · = 6; — · — = 8; — · · — = 10.

RESULTS

Sample volume

Eight different loop volumes (internal and external types) were measured. We obtained the values given in Table I. The actual volumes deviate by up to 39% from the nominal values.

Eluent density

Many SFC controllers offer density programming, based on measurement of pressure and temperature and calculation of densities by means of simple cubic equations of state (EOS), requiring only a few, fluid-specific parameters. We calculated density values for pure carbon dioxide with the Peng–Robinson (PR) EOS model. In the ranges 30–90°C and 100–500 bar the resulting values deviate by up to 9% from reference values (Fig. 2, solid lines). Such a performance is insufficient if eqns. 9 and 10 are to be used for calibration.

For the determination of pure SFC eluent densities, the Bender EOS is much more suitable [9]. This is a 20-parameter modified Benedict–Webb–Rubin EOS. It was adjusted for carbon dioxide by Sievers [10] and deviates by less than 0.5% from reference measurements, except in the vicinity of the critical point.

As we wanted to determine the densities of carbon dioxide with small amounts (up to 10 mol%) of a polar modifier (ethanol), we were seeking EOS models that perform well for this system. We tried a PR EOS model with mixing rules proposed and optimized for carbon dioxide–ethanol by Panagiotopoulos and Reid [7], which performs well in predicting phase boundaries. We calculated densities for various amounts of ethanol (Fig. 2, broken lines; 2–10 mol%) and compared them with densitometric measurements at around 26°C and between 100 and 300 bar. While the PR EOS model predicts increasing densities with increasing ethanol content, measurements (errors ±0.7%) indicate that the eluent densities, in this range, remain virtually unaffected by small contents of ethanol. Hence values calculated with the PR EOS model are generally too high (Fig. 3, closed symbols; deviation *ca.* +7% for 10 mol% ethanol).

As a consequence, we applied the Bender EOS for pure carbon dioxide to calculate eluent densities with less than 8 mol% ethanol. The resulting errors are smaller than 1% in the range 150–300 bar (Fig. 3, open symbols).

UV absorbance of carbon dioxide–ethanol SFC eluents

In order to ascertain the absorbance of the eluents, we measured diode signals and absorption values of carbon dioxide eluents with various contents of ethanol with the LC 235 diode-array detector. Fig. 4 shows that diode signals at different wavelengths above 220 nm do not vary significantly with ethanol contents. At wavelengths below 210 nm however, the carbon dioxide absorbance increases and the ethanol absorbance becomes significant,

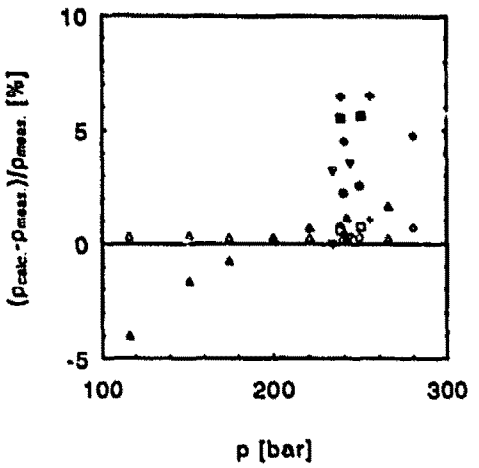

Fig. 3. CO_2–ethanol density: deviation of values calculated with Peng–Robinson EOS (closed symbols) and with Bender EOS (pure CO_2, open symbols) from densitometer measurements at various pressures and compositions ($24.5 < T < 26.7$ C). Ethanol content (%): △, ▲ = 0; ○, ● = 2; ▽, ▼ = 4; ◇, ◆ = 6; □, ■ = 8; +, + = 10.

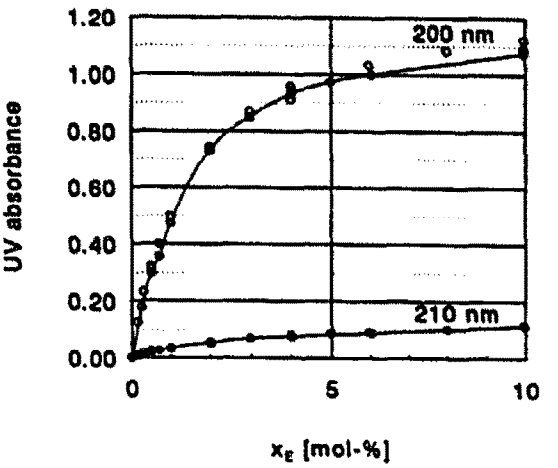

Fig. 5. UV absorbance of CO_2–ethanol eluent (ethanol contents between 0 and 10 mol%) at 200 and 210 nm (33 C, 245 bar).

lowering the diode signals by two decades at 195 nm. At this wavelength, the signal is too weak to distinguish varying ethanol contents. In the normal operating mode, however, the LC235 detector does not give any warning that signals are too weak and erroneous measurements occur.

Fig. 5 shows the absorbances of eluents containing ethanol compared with a pure carbon dioxide eluent. Whereas according to the Lambert–Beer law the dependence of absorbance on ethanol concentration ought to be linear, we find that at low wavelengths (weak detector signals) this is no longer true: at 200 nm the detector response is strongly non-linear.

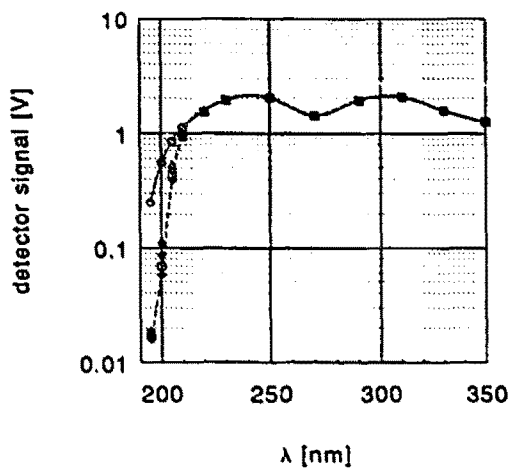

Fig. 4. UV detector diode-array signals at wavelengths between 195 and 350 nm and various ethanol contents of the CO_2 eluent (33 C, 245 bar). Ethanol content (mol%): ○ = 0; △ = 1.986; ▽ = 3.029; □ = 3.976; ◇ = 5.189; + = 5.972.

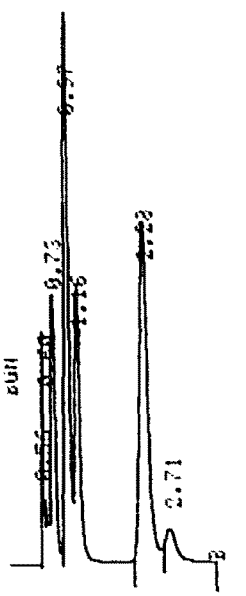

Fig. 6. Separation of underivatized technical grade monoolein (mixture of mono-, di- and triglycerides). Numbers on peaks indicate retention times in minutes. Eluent: CO_2–5.0 mol% ethanol. Column: 34 × 5.3 mm I.D. Nucleosil 100, 3 μm (silica spheres, unmodified); 27 C; eluent density: 929 g l; 0.84 g min CO_2. Detector: Perkin-Elmer LC235, 210 nm.

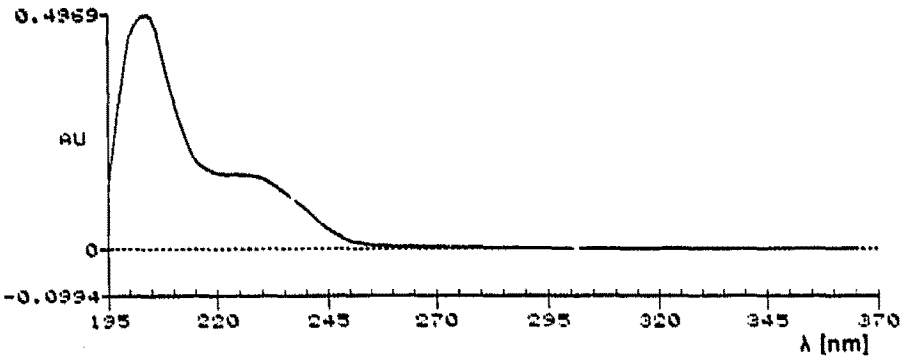

Fig. 7. UV spectrum of 2-monoolein (t = 2.29 min). SFC parameters as in Fig. 6. The "maximum" at 205 nm is an artefact.

Separation and calibration of glycerides

The short columns used in this work performed very well in the separation of underivatized technical-grade monoolein (oleic acid glycerol ester), which is a mixture of about 40% monoglyceride, 40% diglyceride and 16% triglyceride, with small amounts of free glycerol, fatty acids and non-oleic acid esters. Fig. 6 shows a typical chromatogram recorded at 210 nm. According to the spectrum output of the LC235 diode-array detector (Fig. 7), this wavelength ought to be close to the maximum absorbance of oleic acid glycerol esters. Only later did we find that the "maximum" is an artefact due to the above-mentioned weakness of the signals below 210 nm, where the real absorbance continues to increase.

We tried to quantify the results with runs on pure calibration substances. Fig. 8 shows the marked non-linearity of glyceride calibration factors (eqn. 10) at this wavelength. It is not clear whether this is due to the weakness of the signal (non-linear range of the detector) or to measurement too distant from the absorption maximum, where solvent effects and/or eluent absorbance might interfere.

Separation and calibration of tocopherols

Owing to the difficulties with glycerides, we chose substances with a distinct absorbance maximum at longer wavelengths in the UV region. Fig. 9 shows the separation of a solution of α-tocopherol and α-tocopherol acetate at 279 nm with the same short silica cartridge columns utilized throughout this work. A very clear separation of solvent (UV-grade

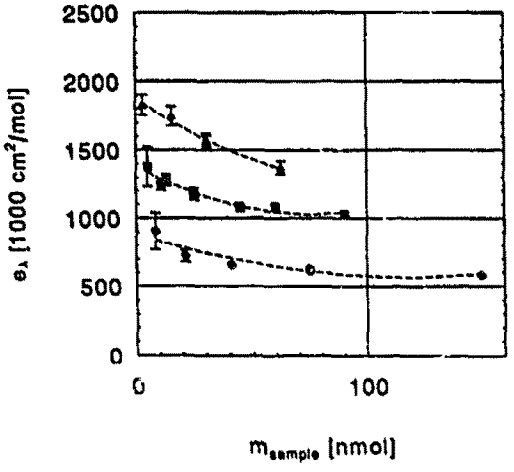

Fig. 8. Calibration factors for (●) mono-, (■) di- and (▲) triglycerides vs. sample size.

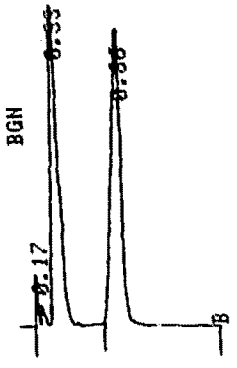

Fig. 9. Separation of α-tocopherol (vitamin E) and α-tocopherol acetate (solution in heptane). Numbers at peaks indicate retention times in minutes. Eluent: CO_2 + 0.5 mol% ethanol. Column: 34 × 5.3 mm I.D. Nucleosil 100, 3 μm (silica spheres, unmodified); 30 C; eluent density: 925 g/l; 2.6 g/min CO_2. Detector: Isco V4, 279 nm.

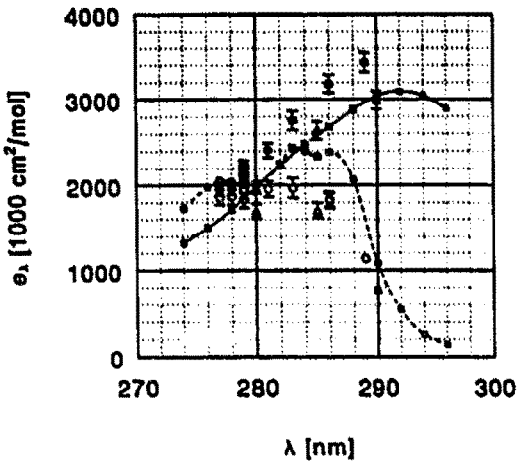

Fig. 10. Comparison between calibration factors of α-tocopherol (vitamin E) (closed symbols) and α-tocopherol acetate (open symbols) determined from (□, ■) literature spectra, (△, ▲) measurements with LC235 detector and (○, ●) measurements with V4 detector.

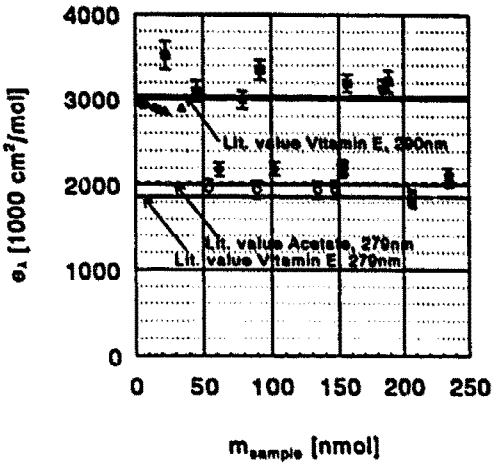

Fig. 11. Calibration factors of α-tocopherol (closed symbols) and α-tocopherol acetate (open symbols) vs. sample size. ○, ● = V4 detector (279 nm); ■ = V4 detector, 290 nm; ▲ = LC235 detector, 290 nm.

heptane), the acetate and tocopherol is achieved with low contents of modifier and a high average column velocity. The detector used initially was the Isco V4.

The values for e_λ calculated from eqn. 10 at first did not match the literature values. Measurements with various wavelengths showed that the V4 detector wavelength selector was maladjusted by 6 nm. Additional measurements with the LC235 detector and comparison with literature data [11] yielded the results presented in Fig. 10.

Whereas the LC235 measurements for α-tocopherol fit the literature curves exactly, the values for acetate are 20–30% below the literature values, although the shape of the spectrum is approximately preserved. After correction of the wavelength readings by −6 nm, the values obtained with the V4 were *ca.* 15% higher than those with the LC235. Its values for tocopherol were higher and those for acetate were lower than the literature values.

As both substances were injected in the same sample solution, and as the absorption maxima match with literature data and the tocopherol values measured by the LC235 always coincided with the literature values, it is assumed that the lower acetate absorbance values are caused by interaction of the SFC eluent.

As the V4 values are consistently higher than the LC235 values for both substances (by 10–15%), the most probable explanation is that the length of the optical path in the V4 detector flow cell is greater than the nominal length by that percentage. This is easily plausible considering the very small path length of only 1 mm. We could not verify this explanation or check whether the deviation is pressure dependent.

Fig. 11 shows a number of measurements made to check the linearity of the detector response with various amounts of sample. Both detectors were used and measurements were taken at two different wavelengths (readings for the V4 detector corrected by −6 nm) and with different SFC operating parameters.

The linearity is satisfactory in the range of measurement error. The deviations below 50 nmol (V4, 290 nm, large error bars) are caused by integration problems due to the very small peaks.

CONCLUSIONS

The method introduced in this paper is well suited for rough calibration of spectrometric detectors in SFC and for approximate comparison of peak values obtained on different detectors at different operating parameters of the SFC. It cuts short the otherwise extensive and time consuming calibration procedure required for relating integrated peak areas to amount of sample if no internal standard method can be used.

It requires a knowledge of molar absorptivity values for the analyte substances and an SFC system with stable, reproducible flow and equipment for the determination of mass flow-rate and density in the detector flow cell, in addition to its optical path length.

These prerequisites are met neither easily nor cheaply (hardware requirements). Deviations from literature values and among the values measured with the two detectors (Fig. 11) show that it is not straightforward to apply the method and obtain accurate quantitative results. Under normal laboratory conditions it is difficult to measure the optical path length of the detector cell and to judge solvent effects of SFC eluents on the UV spectra of samples. For these reasons, the time-consuming calibration procedures described here will still be required if accurate quantitation is to be achieved.

SYMBOLS

A	Optical absorbance
a_i	Peak area (integrated)
c	Concentration
E	Exit age distribution
e	Calibration factor
F	Normalized outlet (response) function of an inlet step function
I	Light intensity
l_0	Optical path length
$\dot{m}$	Mass flow-rate
n	Number of moles of sample
R	Residence time distribution
t	Time
V	Volume
$\dot{V}$	Volume flow-rate

Greek letters

ε	Molar absorptivity
λ	Wavelength
ρ	Density
τ	Mean residence time

Subscripts

fc	Flow cell
i	Integrated
meas.	Measured

ACKNOWLEDGEMENTS

We thank the Swiss Federal Institute of Technology (ETH), Zurich, the Basle Chemical Industry Fonds and the Emil Barell Foundation for sponsoring this research project.

REFERENCES

1 W. Pipkin, *LC · GC Int.*, 5 (1992) 8–10.
2 U. Meier, *Dissertation*, No. 9756, ETH, Zurich, 1992.
3 G. Torsi, G. Chiavari, C. Laghi, A. M. Asmundsdottir, F. Fagioli and R. Vecchietti, *J. Chromatogr.*, 482 (1989) 207–214.
4 G. Torsi, G. Chiavari and M. T. Lippolis, *LC · GC Int.*, 5 (1992) 37–39.
5 K. Peck and M. D. Morris, *J. Chromatogr.*, 448 (1988) 193–201.
6 R. D. Smith, in M. Yoshioka (Editor), *SFC and Micro-HPLC*, VSP, Utrecht, 1989, Ch. 2.1.
7 A. Z. Panagiotopoulos and R. C. Reid, in Th. G. Squires and M. E. Pauliatis, *High-pressure phase equilibria in ternary fluid mixtures with a supercritical component (ACS Symposium Series*, No. 329), American Chemical Society, Washington, DC, 1987, pp. 115–121.
8 O. Levenspiel, *Chemical Reaction Engineering*, Wiley, New York, 2nd ed., 1972, Ch. 9.
9 U. Sievers, *Chem.-Ing.-Tech.*, 58 (1986) 220.
10 U. Sievers, *Fortschr. Ber. VDI Z., Reihe* 6, 155 (1984) 8.
11 *Sadtler's Atlas of UV Spectra*, Sadtler Research Laboratories, Philadelphia, PA, No. 20771 UV, 1973, and 2780 UV, 1975.